ORGANIC CHEMISTRY

FRONTIERS

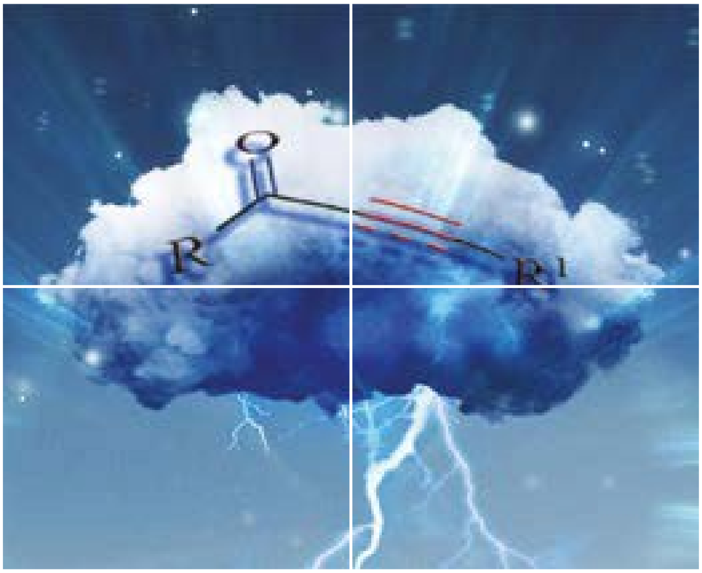

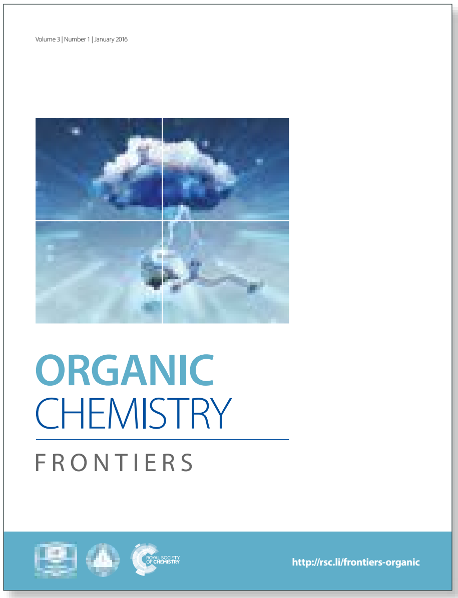

Organic Chemistry Frontiers

RESEARCH ARTICLE

Polymerization of Acetylene: Polyynes, but not Carbyne[†,‡]

Dominik Prenzel,[a] Rolf W. Kirschbaum,[b] Wesley A. Chalifoux,[c] Robert McDonald,[d] Michael J. Ferguson,[d] Thomas Drewello,[b] and Rik R. Tykwinski[a,d,*]

Received 00th January 20xx,
Accepted 00th January 20xx

DOI: 10.1039/x0xx00000x

www.rsc.org/

The formation of polyynes *via* polymerization of acetylene gas and endcapping with tris(3,5-di-*t*-butylphenyl)methyl moiety (Tr*, supertrityl) has been explored. The polymerization process has been optimized based on the length of the polyyne endcapping groups. Separation-purification-identification has been achieved through reversed-phase (RP) high performance liquid chromatography (HPLC), utilizing UV-vis detection, which offers UV-vis spectra of the polyyne products. The chain length of individual polyynes can then be established through comparison to the spectra trends of known polyyne samples. LDI and MALDI mass spectrometry is used to examine the presence of **Tr*[*n*]** polyynes in the crude reaction mixture. The combined analyses show that polymerization reactions of acetylene using the supertrityl endgroup allow formation of polyynes, but much shorter than could be achieved by stepwise syntheses.

Introduction

In the past few years, there has been a growing fascination with the synthesis of materials formed from carbon – the allotropes.[1] On the basis of the hybridization state of carbon, the allotrope composed of only *sp*-hybridized carbon atoms would be carbyne.[2] Carbyne is predicted to have a quasi one-dimensional, rod-like structure, consisting of either alternating single and triple bonds to give a polyynic structure, or consecutive double bonds resulting in a cumulenic structure (Fig. 1a).[2–6]

As a material, carbyne has recently generated excitement particularly due to theoretical predictions of unprecedented mechanical and electronic properties.[7] As potential uses for carbyne increase, there is a concurrent focus on producing macroscopic quantities. The formation of “bulk” polyynic material by either gas-phase deposition techniques[7–10] or laser ablation[11–14] has been investigated extensively since the beginning of the 21st century. Despite these efforts, there remains little evidence that carbyne has truly been formed and characterized.[15] As model systems, polyynes and cumulenes (also called carbon atom wires, CAWs[16]), have been used to approximate some of the desired properties of carbyne.[2–6,17] The most difficult challenge facing the study of carbyne-like materials is typically their tendency to decompose or polymerize. On the other hand, decomposition can often be circumvented by placing sterically demanding endgroups at the termini of the carbon chains (Fig. 1a). Using this approach the longest polyyne characterized to date consists of 22 conjugated triple bonds,[2] endcapped with the tris(3,5-di-*t*-butylphenyl)methyl moiety (Tr*, supertrityl, Fig. 1b). Conversely, the longest reported cumulenic model compound

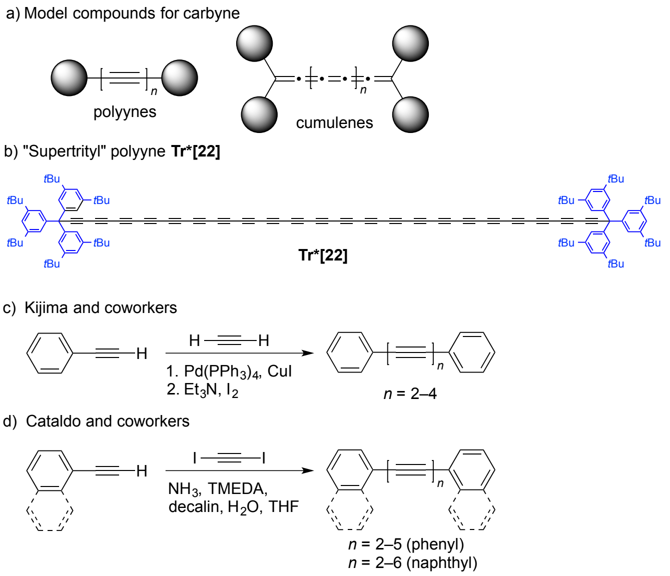

Fig. 1 (a) Schematic structures of polyynes and cumulenes as models for carbyne, with sterically demanding endgroups, (b) Chemical structure of the longest known polyyne **Tr*[22]**, with Tr* endgroup shown in blue, and polymerization protocols toward carbyne (and achieved chain lengths *n*) reported by (c) Kijima and (d) Cataldo.

---

[a] *Institut für Organische Chemie I, Friedrich-Alexander-Universität Erlangen-Nürnberg, Henkestrasse 42, 91054 Erlangen, Germany.*
E-mail: rik.tykwinski@fau.de
[b] *Institut für Physikalische Chemie I, Friedrich-Alexander-Universität Erlangen-Nürnberg, Egerlandstrasse 3, 91058 Erlangen, Germany.*
[c] *Department of Chemistry, University of Nevada, 1664 N. Virginia St., Reno, NV 89557, USA.*
[d] *Department of Chemistry, University of Alberta, 11227 Saskatchewan Drive NW, Edmonton, Alberta, T6G 2G2, Canada.*
[e] *E-mail: rik.tykwinski@ualberta.ca*

† Electronic Supplementary Information (ESI) available: Experimental Section, IR, UV-vis, and (MA)LDI spectra, and detailed X-ray crystallographic data in CIF format. CCDC 1507657–1507659. See DOI: 10.1039/x0xx00000x

‡ Dedicated in the memory of Sir Harold Kroto

for carbyne is much shorter and consists of 9 cumulated double bonds (a [9]cumulene).[18,19] In both of these cases, a stepwise synthesis is used to achieve the desired polyyne(s) and cumulene(s), which allows both the endgroup and chain length to be defined from the outset. The disadvantage of a stepwise synthesis is, of course, the numerous synthetic transformations needed for each molecule are often tedious, expensive, and time consuming.

There have been a number of attempts to synthesize carbyne through polymerization reactions, using, for example, acetylene gas,[20–22] lithium bromoacetylide (Li–C≡C–Br),[23] or diiodoacetylene.[24–26] For example, Kijima and coworkers[27] attempted the polymerization of acetylene in the presence of a small amount of phenylacetylene as an end-capping agent (Fig. 1c), with a Pd / Cu catalyst system under mild anaerobic conditions. The Kijima protocol gave polyynes from diyne to tetrayne (i. e., n = 2 – 4, where n = number of acetylenic units). Cataldo and coworkers also used phenyl acetylene as an endcapping group,[28] as well as 1-naphthyl acetylene (Fig. 1d).[29] The Cataldo approach relied on diiodoacetylene as the sp-carbon building block, and this study identified polyynes ranging from diyne to hexayne.

Thus, while acetylene offers a low-cost and reactive precursor to form polyynes in a one-pot synthesis, existing approaches have led to mixtures of products that are limited in length and can be difficult to purify and / or characterize. We hypothesized that perhaps the choice of endcapping group played a role in the limited success of previous reports. Namely, it is well established that aryl endcapped polyynes are typically unstable in solution by the length of an octa- or decayne, and that terminal acetylenes (i.e., polyynes terminate at one end with –H) bearing aryl groups are even less stable (and even explosive).[30] In other words, it is possible, and even likely, that longer polyynes were not identified via the Kijima and Cataldo protocols because the products and intermediates were not stable.

We predicted that a larger, more sterically "protecting" endgroup would give more satisfying results. The supertrityl endcapping group for polyynes (Tr*, Fig. 1b), first introduced in 2010,[2] has achieved this goal. Even in the case of terminal acetylenes, earlier work has shown that the Tr* group provides rather amazing results, and molecules up to the terminal Tr*-heptayne could be isolated without significant decomposition. Thus, it seems reasonable that the Tr* group would offer the best option for the investigating and developing a general procedure to carbyne/polyynes based on acetylene polymerization. We report herein our efforts to realize carbyne/polyynes through acetylene polymerization using Tr* as an endcapping group, and we confirm that this approach is not suitable for the formation of carbyne-like materials, even under optimized conditions.

Results and Discussion

For our polymerization reactions, we chose to use a method inspired by the established procedure of Kijima and coworkers (Scheme 1).[27] As an oxidant, I_2 can be used, although we also explored ethyl bromoacetate (EBA) since our previous work had shown improved yields in comparison to I_2 in Pd/Cu-catalysed oxidative coupling reactions.[31] Acetylene gas (for purification procedure, see Fig. S1) was chosen as the carbon source.

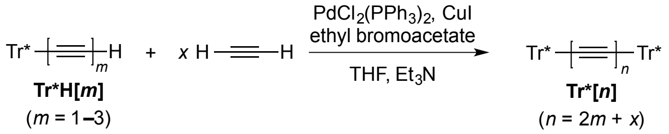

Scheme 1 General reaction scheme for the polymerization of acetylene with endcapping groups **Tr*H[1–3]**.

Three Tr*-endcapping groups with differing polyyne lengths were considered, namely **Tr*H[1]**, **Tr*H[2]**, and **Tr*H[3]** (Fig. 2). There were three major considerations with respect to the endgroup. The first consideration was the synthetic stability and accessibility of the species used as the endcapping group (**Tr*H[*m*]**), which has been demonstrated to be excellent for all three derivatives.[2] Second, we considered the reactivity of **Tr*H[*m*]** in the oxidative acetylenic polymerization reaction, which should be dictated by the acidity of the alkynyl proton. Hence, reactivity should increase as a function of length from **Tr*H[1]** through to **Tr*H[3]**.[32] Finally, there would be a significant influence on the polymerization arising from steric hindrance at the reaction centre from the Tr* group. Based on X-ray crystallographic characterization, this would be substantial for reaction of **Tr*H[1]**, and then decrease as a function of length from **Tr*H[2]** to **Tr*H[3]** (Fig. 2). The X-ray crystallographic analysis also showed slight trends in alkyne

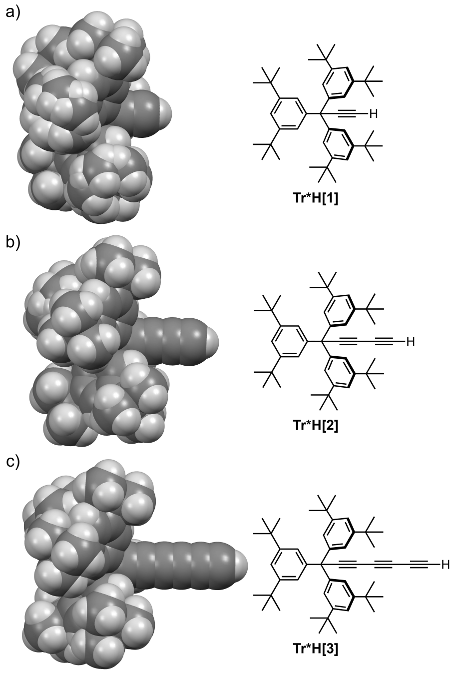

Fig. 2 X-ray crystallographic results (space-filling rendering) and chemical structures of (a) **Tr*H[1]**, (b) **Tr*H[2]**, and (c) **Tr*H[3]** highlighting the steric hindrance resulting from the Tr* group.

bond lengths as a function of molecular length,[33] which are described in Table S1.[34]

Of the three factors described above, the reactivity of the endcapping group was deemed vital in order to achieve long polyynes. Empirically, the rate of incorporating acetylene groups giving rise to chain elongation (k_1, eq 1) would be expected to occur mainly through a process best described as chain-growth (based on the excess of acetylene). Alternatively, chain elongation could also be achieved through the formation of polyynes **H[*n*]** (k_2, eq 2), a likely and desirable process facilitated by a huge excess of acetylene. The **H[*n*]** species should, ideally, be endcapped relatively early (k_3, eq 3), since longer **H[*n*]** species are expected to decompose even in solution.[5a,9,35,36] If the rate of chain elongation (namely k_1 & k_3) is initially higher than that of homocoupling of **Tr*H[m]** and **Tr*H[y]** (k_4, eq 4), then longer polyynes would be formed. Thus, the most favourable situation would be k_1 & $k_3 \geq k_2 >> k_4$.[37]

In initial experiments (see Supporting Information), the monoyne (**Tr*H[1]**) was used as the endcapping reagent in the presence of excess acetylene, $PdCl_2(PPh_3)_2$, CuI, and EBA, in keeping with previously reported procedure of Kijima and coworkers (Scheme 1).[27] Unfortunately, the chain growth with **Tr*H[1]** was seemingly slow, and the reaction resulted mostly in black, insoluble solids; presumably polymerized and decomposed acetylene (i. e., $k_2 >> k_1$), as assessed by IR and UV-vis spectroscopy (Fig. S2 and S3). To increase the reactivity of the endcapping group, **Tr*H[2]** was used, and this resulted in products with a few absorptions in the lower energy region of the UV-vis spectrum (Fig. S4), indicating a small concentration of longer, stable polyynes had been formed. Nevertheless, the reaction remained less than ideal.

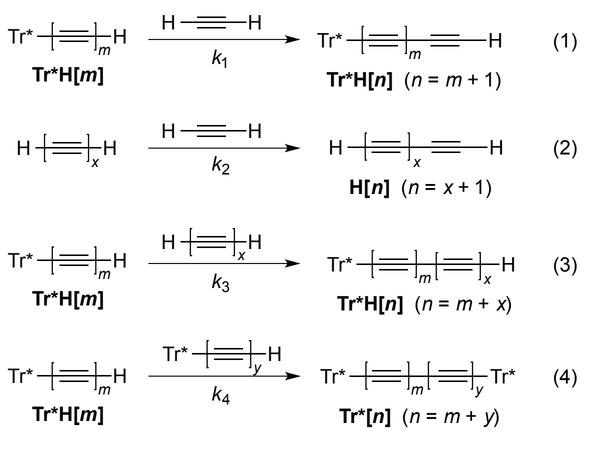

Initial polymerization with **Tr*H[3],** on the other hand, gave a reproducible protocol that formed long polyynes **Tr*[n]**. Several variations of the reaction using **Tr*H[3]** were explored. Under N_2 atmosphere, $PdCl_2(PPh_3)_2$ and CuI were dissolved in dry THF, followed by the addition of Et_3N and then EBA. Acetylene gas was bubbled through the stirring solution for 10 min to initiate acetylene polymerization (i. e., eq 2). Compound **Tr*H[3]** dissolved in dry THF was added dropwise over 1 h to favour polyyne chain length grow (i. e., eq 1). Bubbling of acetylene gas into the solution was continued in order to maintain an excess of acetylene gas and reduce the possibility of homocoupling (eq 4). After ca. 1 hr, a black precipitate began to form, presumable via **H[*n*]** formation and decomposition as described in eq 2. At this point, the reaction was judged “complete”, and N_2 was bubbled through the reaction mixture for 10 min to remove unreacted acetylene.[38] The reaction was stirred at rt for 16 h and an additional portion of EBA was added to promote completion of the homocoupling reaction to give the desired **Tr*[*n*]** polyynes. The reaction was quenched, the mixture extracted with hexanes, washed with brine, dried over $MgSO_4$, and the solvent concentrated under reduced pressure to about 30 mL. This solution was passed through a small pad of silica gel with hexanes to remove all intractable material. The filtrate was concentrated to approximately 30 mL to give **Sample A** that was used for analyses (*vide infra*).

The analogous reaction sequence described for **Sample A** was also repeated using iodine instead of ethyl bromoacetate as the oxidant (i. e., the original conditions reported by Kijima and coworkers).[27] Work up of the reaction consisted of washing with a solution of saturated aqueous $Na_2S_2O_3$ to remove excess I_2, followed by washing with brine, and concentration under reduced pressure to about 30 mL. This solution was then passed through a small pad of silica gel with hexanes. The filtrate was concentrated to approximately 50 mL, resulting in a product solution in hexanes, **Sample B**, which was used for analyses.

UV-vis spectroscopy is a potent tool for characterization of **Tr*[*n*]** polyynes due to the very distinct absorption bands these compounds show, including the vibrational fine structure.[2] Absorbances for **Tr*[*n*]** polyynes also show a predictable bathochromic shift as a function of chain length that reflects extension of the conjugated π-system, and this spectroscopic trend offers the possibility to correlate the lowest energy absorption (λ_{max}) to the chain length of particular molecules as shown in Fig. 3.[2,39–42] The trend shown in Fig. 3 is derived from the experimentally obtained data for

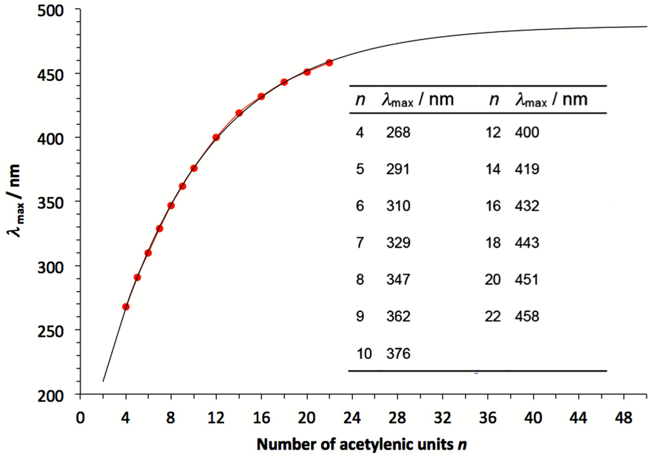

n	λ_{max} / nm	n	λ_{max} / nm
4	268	12	400
5	291	14	419
6	310	16	432
7	329	18	443
8	347	20	451
9	362	22	458
10	376		

Fig. 3 Convergence of the absorption maxima for **Tr*H[*n*]** polyynes according to eq 5 with data using the longest wavelength absorbance (λ_{max}) for known derivatives measured in hexanes (λ_{max} values from references 2 and 39).

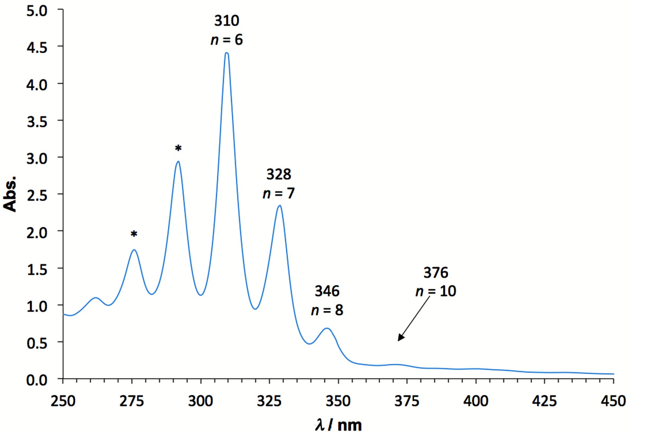

Fig. 4 Qualitative UV-vis spectrum of **Sample A**, displaying λ_{max}/nm and corresponding n values (* signals corresponding values of vibrational fine structure of **Tr*[6]**).

Tr*[*n*] polyynes[2,39] using the approach of Meier and coworkers,[43] and accounts for the fact that at some length polyynes will reach an effective conjugation length (i. e., constant $\lambda_{(n)}$ value versus length) *via* the relationship:

$$\lambda_{(n)} = \lambda_{\infty} - (\lambda_{\infty} - \lambda_1)e^{-a(n-1)} \qquad (5)$$

where $\lambda_{(n)}$ is λ_{max} for a polyyne **Tr*[*n*]** of length n, λ_1 = 176 nm, λ_{∞} = 487 nm is the limiting value as $n \rightarrow \infty$, and the parameter a = 0.114 gives an indication of how fast saturation (convergence) is approached. With eq 5 in hand, it is possible to calculate the chain lengths of unknown **Tr*[*n*]** polyynes from an experimentally determined λ_{max}-value.

The UV-vis spectrum of **Sample A** (Fig. 4) reveals clear absorbances at wavelengths that are consistent with **Tr*[*n*]** polyynes with chain lengths of n = 6, 7, 8, and 10. Analysis of the crude product mixture of **Sample A** *via* (MA)LDI mass spectrometry, on the other hand, did not show signals consistent with **Tr*[*n*]** products (Fig. S7). This result was quite surprising, since MALDI MS has been used previously to characterize pure samples of **Tr*[*n*]** polyynes of analogous length.[44] We assume that the crude mixture contained other components that prevented ion formation of **Tr*[*n*]** polyynes and / or the transfer into the gas phase.

The UV-vis spectrum of **Sample B** showed no distinguishing features relative to **Sample A**, aside from a weak absorption at 520 nm, presumably arising from unreacted iodine,[45] and perhaps a slight increase in ratio of longer polyynes (n = 8, 10, see Fig. S5) in comparison to **Sample A**. Analysis of **Sample B** by (MA)LDI MS (especially LDI) in the negative-ion mode, on the other hand, revealed regular patterns of a multitude of polyyne anions including **Tr*[6]**, **Tr*[7]** and **Tr*[8]** (Fig. 5). In comparison to **Sample A**, it is possible that residual iodine provides a softer ionization/desorption process for the polyynes,[46] and/or lowers the energy thresholds for ion formation in MALDI.[47]

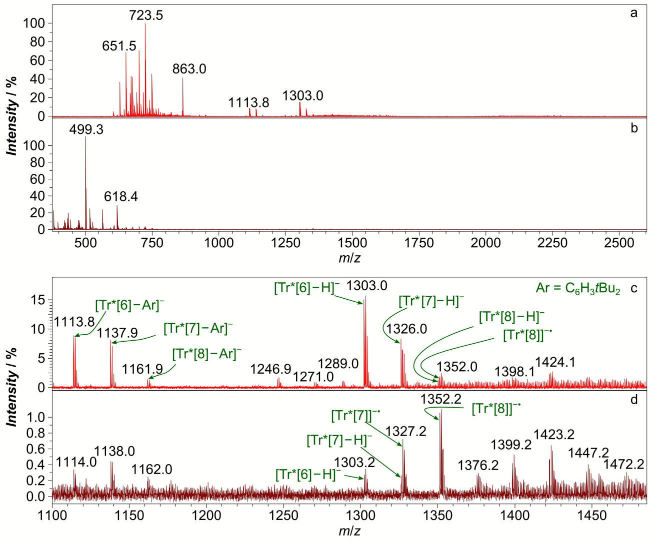

Fig. 5 Top: MS analysis of **Sample B**, showing a) an LDI-TOF mass spectrum (negative-ion mode) of a dried droplet of the product solution and b) a MALDI-TOF mass spectrum (negative-ion mode) of the product solution mixed with *trans*-2-[3-(4-*t*-butylphenyl)-2-methyl-2-propenylidene]malononitrile (DCTB)[48] dissolved in dichloromethane (DCM). Matrix / analyte ≈ 10^3 : 1 (mol/mol). Bottom: Expansions of the same spectra, c) the LDI and d) the MALDI, each indicating the presence of deprotonated polyynes **[Tr*[*n*]** – H]$^-$ and / or the radical anion species **[Tr*[*n*]]**$^{-\bullet}$ with n = 6 – 8.

Specifically, the LDI-TOF spectra of **Sample B** (Figs. 5a and 5c) show signals at m/z 1303.0, 1326.0 and 1352.0 (each m/z referring to the highest peak of the isotope envelope), which are assigned to **[Tr*[6]** – H]$^-$, **[Tr*[7]** – H]$^-$, and **[Tr*[8]]**$^{-\bullet}$ / **[Tr*[8]** – H]$^-$. Complementing the LDI analysis, MALDI-TOF spectra (Fig. 5b and 5d) were acquired using *trans*-2-[3-(4-*t*-butylphenyl)-2-methyl-2-propenylidene]-malononitrile, DCTB[48] as a matrix (with a matrix-to-analyte ratio estimated to 1000 : 1). The MALDI signals at m/z 1303.2, 1326.2, and 1352.2 are assigned to **[Tr*[6]** – H]$^-$, **[Tr*[7]]**$^{-\bullet}$ / **[Tr*[7]** – H]$^-$, and **[Tr*[8]]**$^{-\bullet}$. This is in accordance with the deprotonation behaviour of Tr* endcapped polyynes under LDI and MALDI conditions, respectively. Experiments with pure, monodisperse compounds having a known number of *sp*-carbon atoms showed that the degree of formal deprotonation/elimination (i. e., the intensity ratio of the deprotonated polyyne to the radical anion) decreases with an increasing *sp*-carbon chain length in the negative-ion mode (Fig. S8). The loss of the neutral fragment $C_6H_3tBu_2$ (189 u) from the polyyne anion is typically observed under LDI conditions. The corresponding charged fragments **[Tr*[6]** – $C_6H_3tBu_2$]$^-$, **[Tr*[7]** – $C_6H_3tBu_2$]$^-$, and **[Tr*[8]** – $C_6H_3tBu_2$]$^-$ of the polyyne anions with n = 6, 7, and 8 are detected at m/z 1113.8, 1137.9, and 1161.9. Peaks observed at m/z 1376.2, 1399.2, 1423.2, 1447.2, and 1472.2 nearly fit the masses of **Tr*[9]**, **Tr*[10]**, **Tr*[11]**, **Tr*[12]**, and **Tr*[13]**. However, the signals indicate either deprotonation of the product or the signal-to-noise ratio is too weak to determine the first peak of the isotope pattern (i. e., to distinguish between the deprotonated polyyne and the radical anion). On the basis of control measurements, deprotonation is not expected for chain lengths greater than n = 9 (see Fig.

S8), which is not consistent with observed series of signals between *m*/*z* 1376.2 and 1472.2. Therefore, the above-mentioned signals cannot be unequivocally assigned to **Tr*[*n*]** polyynes where *n* = 9 to *n* = 13. Additionally, MALDI measurements with equimolar mixtures of **Tr*[*n*]** polyynes of different chain lengths show that the ionization/desorption process of longer polyynes is preferred over shorter polyynes resulting in higher intensities for the longer polyynes (Fig. S6). This makes it impossible to detect all polyynes present in a bulk solution, especially if the chain lengths differ by more than two carbon-carbon triple bonds. Thus, the MS data unequivocally establishes the formation of **Tr*[*n*]** with *n* = 6, 7, and 8, but the identity of members of the ion series between *m*/*z* 1376.2 and *m*/*z* 1472.2 could not be conclusively established with the employed instrumentation.

Toward the separation, isolation, and characterization of individual **Tr*[*n*]** polyynes from the polymerization reactions, analytical HPLC was explored using **Sample A** and a normal phase column (SiO_2 / hexanes) in combination with low flow rates (0.05 mL / min). The separation was monitored *via* a UV-vis photodiode array detector (DAD)[9,22] and showed some separation of the polyyne mixture. Unfortunately, however, complete separation was not possible although polyynes could be enriched. Fig. 6a shows the corresponding two-dimensional chromatogram of **Sample A**, namely the detection wavelength from DAD as a function of the retention time. The contour plot represents absorption intensity of the chemical species under analysis, and each group of vertically aligned spots at a particular retention time corresponds to the UV-vis absorptions of the matching polyyne. The signals appear over approximately one hour, but the difference in polarity of the **Tr*[*n*]** polyynes is not sufficient for normal phase HPLC to effect a clean separation. Despite these limitations, there was evidence for the formation of polyynes with chain lengths even longer than *n* = 10, with absorbances observed at $\lambda > 370$ nm.

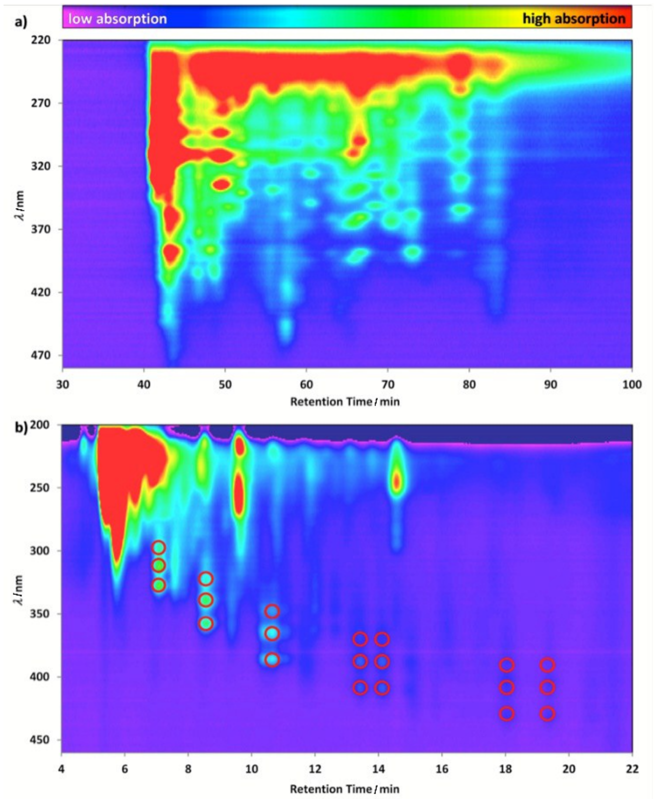

Fig. 6 (a) 2D-HPLC (DAD) chromatogram of **Sample A** (200 μL, hexanes @ 0.05 mL / min) showing the separation of **Tr*[*n*]** polyynes. The detection wavelength for the UV absorption (contour) as a function of the retention time. (b) 2D-RP-HPLC (DAD) chromatogram of **Sample C** (200 μL, CH_3CN / H_2O 80:20 @ 0.5 mL / min). The red circles mark the characteristic signature for the separated polyynes shown in Fig. 7.

Alternatively, HPLC using a RP-C_{18} column and polar mobile phase (200 μL / run, CH_3CN / H_2O 80:20 v/v) showed improved separation of the **Tr*[*n*]** mixture. The native form of **Sample A**, however, could not be used due to insolubility of the sample in the eluent. For the RP-HPLC procedure, **Sample A** (20 mL) was diluted with CH_3CN (50 mL) and then with Et_2O (20 mL) to enhance phase mixing. The Et_2O and hexanes were removed under reduced pressure, giving a heterogeneous mixture in CH_3CN (ca. 50 mL). A brown precipitate formed after the solution was left standing for 1 d in CH_3CN and was removed by filtration through a small pad of silica gel with CH_3CN. The resulting yellow filtrate was concentrated to ca. 10 mL to give **Sample C**. RP-HPLC separation of **Sample C** (200 μL / run, CH_3CN / H_2O 80:20 v/v) was improved by a higher flow rate/pressure, and the time for one run was reduced to ca. 20 min. Shorter polyynes eluted first, followed by longer polyynes, as can be seen in the chromatogram in Fig. 6b. For longer polyynes, separation was clearly not complete, with multiple samples showing similar absorption profiles. Nevertheless, the distinct absorption bands allowed empirical determination of polyyne length based on the trend in Fig. 3.[49] Using the DAD, the UV-vis spectra of **Tr*[*n*]** polyynes with *n* = 7, 11, 13, and 16 could be identified from **Sample C** (Fig. 7), and the λ_{max} values fit to the reported/predicted values with variance ≤ 2 nm. The spectrum from the sample with a retention time of 8.53 min is tentatively assigned to **Tr*[*n*]** with *n* = 8 or *n* = 9, as it lies between the expected λ_{max} values for these two polyynes.[49] Thus, RP-HPLC coupled with DAD provides strong evidence for the formation of **Tr*[*n*]** polyynes *via* UV-vis analysis, but, unfortunately, this analysis does not allow for even a crude estimation of the reaction yield. It is interesting to note at this point that the RP-HPLC / DAD analysis suggests a higher proportion of products with an odd number of acetylene units. While such an outcome would be desirable in view of the difficulties often encountered in the synthesis of "odd" polyynes, the origin of the trend observed in the current study remains unknown.

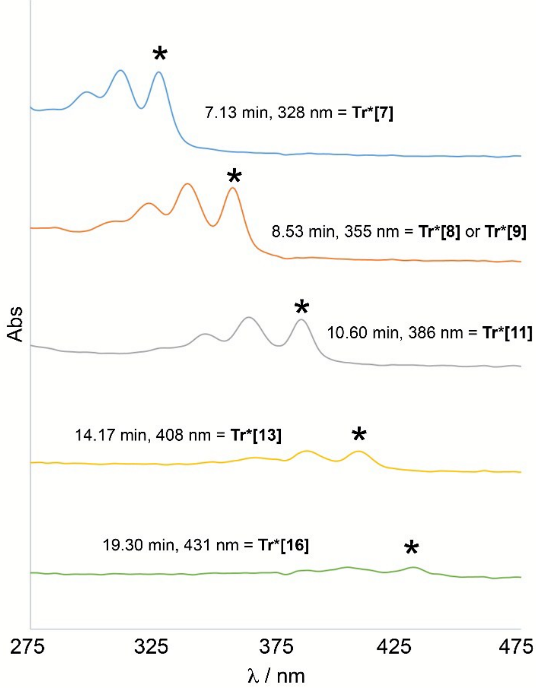

Fig. 7 RP-HPLC (DAD) UV-vis spectra of **Sample C**, containing polyynes **Tr*[7]** (blue), **Tr*[11]** (grey), **Tr*[13]** (yellow), and **Tr*[16]** (green) with corresponding λ_{max} values and retention times.

Conclusions

We have shown by UV-vis analysis as well as (MA)LDI MS and RP-HPLC that **Tr*[*n*]** polyynes up to at least *n* = 16 are formed during polymerization reactions with acetylene and **Tr*H[1–3]** endcapping groups. In spite of the well-documented stabilizing and solubilizing effects for the supertrityl endgoups Tr*, significant challenges are encountered in preparative separation of the **Tr*[*n*]** products. We have, however, demonstrated that RP-HPLC can be a potent analytical tool for separation of **Tr*[*n*]**-polyyne mixtures and identification *via* UV-vis spectroscopy/DAD.

Arguably, the most significant conclusion from our studies is the possibility that the polymerization of acetylene might not offer a facile route to carbyne-like materials. While we form shorter polyynes (*n* up to ca. 10, a decayne) under optimized conditions (as previously demonstrated by e.g., Kijima and Cataldo with analogous procedures), longer polyynes are not observed in significant quantities. Given that the supertrityl moiety (Tr*) should offer the best possible stabilization for extended polyynes, our inability to form long polyynes demonstrates that the polymerization of acetylene is probably the weak link in the process, rather than instability of the polyyne products. Thus, our quest to form carbyne will continue with a focus on alternative catalysts and reaction conditions.

Acknowledgements

Funding from the University of Erlangen-Nuremberg and the Deutsche Forschungsgemeinschaft (DFG – SFB 953, ‘‘Synthetic Carbon Allotropes’’) is gratefully acknowledged.

Caution

The instability of polyynes can be significant, especially those without endcapping groups (so called terminal polyynes), and one should therefore handle all polyynes with care. As solids, terminal polyynes should be regarded as potentially explosive, even with the exclusion of air. Polyynes can be especially dangerous under any type of heating or pressure, and “scraping” of a solid polyyne product out of a round bottom flask with a metal spatula should be avoided or done with extreme caution and safety precautions.

Notes and references

1 A. Hirsch, *Nat. Mater.*, 2010, **9**, 868.
2 W. A. Chalifoux and R. R. Tykwinski, *Nat. Chem.,* 2010, **2**, 967.
3 M. Jevric and M. B. Nielsen, *Asian J. Org. Chem.*, 2015, **4**, 286.
4 Y. Tobe and T. Wakabayashi in *Acetylene Chemistry*, ed. F. Diederich, P. J. Stang and R. R. Tykwinski, Wiley-VCH, Weinheim, 2005, chapter 9.
5 a) W. A. Chalifoux and R. R. Tykwinski, *C. R. Chim.*, 2009, **12**, 341; b) W. A. Chalifoux and R. R. Tykwinski, *Chem. Rec.*, 2006, **6**, 169.
6 J. A. Januszewski and R. R. Tykwinski, *Chem. Soc. Rev.*, 2014, **43**, 3184.
7 M. Liu, V. I. Artyukhov, H. Lee, F. Xu and B. I. Yakobson, *ACS Nano*, 2013, **7**, 10075. V. I. Artyukhov, M. Liu and B. I. Yakobson, *Nano Letters*, 2014, **14**, 4224
8 *Polyynes: Synthesis, Properties, and Applications*, F. Cataldo ed., Taylor & Francis, Boca Raton, FL, 2006.
9 a) F. Cataldo, *Carbon*, 2003, **41**, 2671; b) F. Cataldo, *Carbon*, 2004, **42**, 129.
10 L. Ravagnan, P. Piseri, M. Bruzzi, S. Miglio, G. Bongiorno, A. Baserga, C. S. Casari, A. Li Bassi, C. Lenardi, Y. Yamaguchi, T. Wakabayashi, C. E. Bottani and P. Milani, *Phys. Rev. Lett.*, 2007, **98**, 216103.
11 M. Tsuji, S. Kuboyama, T. Matsuzaki and T. Tsuji, *Carbon*, 2003, **41**, 2141.
12 H. Tabata, M. Fujii and S. Hayashi, *Carbon*, 2006, **44**, 522.
13 Y. Taguchi, H. Endo, Y. Abe, J. Matsumoto, T. Wakabayashi, T. Kodama, Y. Achiba and H. Shiromaru, *Carbon*, 2015, **94**, 124.
14 A. Hu, M. Rybachuk, Q.-B. Lu and W. W. Duley, *Appl. Phys. Lett.*, 2007, **91**, 131906.
15 P. Tarakeshwar, P. R. Buseck and H. W. Kroto, *J. Phys. Chem. Lett.*, 2016, **7**, 1675.
16 C. S. Casari, M. Tommasini, R. R. Tykwinski and A. Milani, *Nanoscale*, 2016, **8**, 4414.
17 R. R. Tykwinski, *Chem. Rec.*, 2015, **15**, 1060.
18 J. A. Januszewski, D. Wendinger, C. D. Methfessel, F. Hampel and R. R. Tykwinski, *Angew. Chem. Int. Ed.*, 2013, **52**, 1817.
19 M. Franz, J. A. Januszewski, D. Wendinger, C. Neiss, L. D. Movsisyan, F. Hampel, H. L. Anderson, A. Görling and R. R. Tykwinski, *Angew. Chem. Int. Ed.*, 2015, **54**, 6645.
20 W. J. Gensler, *Chem. Rev.*, 1957, **57**, 191.
21 V. V. Korshak, V. I. Kasatochkin, A. M. Sladkov, Y. P. Kudryavtsev and K. Usenbaev, *Dokl. Akad. Nauk SSSR*, 1961, **136**, 1342; A. M. Sladkov, *Sov. Sci. Rev., Sect. B*, 1981, **3**, 75.
22 F. Cataldo, *Polym. Int.,* 1999, **48**, 15.

23 Lagow and coworkers reported that very long polyynes were produced from a polymerization procedure, but the characterization of these products does not seem to fully justify their claims, see: R. J. Lagow, J. J. Kampa, H.-C. Wei, S. L. Battle, J. W. Gegne, D. A. Laude, C. J. Harper, R. Bau, R. C. Stevens, J. F. Haw and E. Munson, *Science*, 1995, **267**, 362.

24 T. Yamamoto, *Prog. Polym. Sci.*, 1992, **17**, 1153.

25 M. Kijima, Y. Sakai and H. Shirakawa, *Chem. Lett.*, 1994, **23**, 2011.

26 M. Kijima, Y. Sakai and H. Shirakawa, *Synth. Met.*, 1995, **71**, 1837.

27 T. Hattori, M. Kijima and H. Shirakawa, *Synth. Met.*, 1997, **84**, 357.

28 F. Cataldo, O. Ursini , G. Angelini , M. Tommasini and C. Casari, *J. Macromol. Sci. A*, 2010, **47**, 739.

29 F. Cataldo, L. Ravagnan, E. Cinquanta, I. E. Castelli, N. Manini, G. Onida and P. Milani, *J. Phys. Chem. B*, 2010, **114**, 14834.

30 T. Luu, E. Elliott, A. D. Slepkov, S. Eisler, R. McDonald, F. A. Hegmann and R. R. Tykwinski, *Org. Lett.*, 2005, **7**, 51; see also J. B. Armitage, N. Entwistle, E. R. H. Jones and M. C. Whiting, *J. Chem. Soc.,* 1954, 147.

31 W. A. Chalifoux, M. J. Ferguson and R. R. Tykwinski, *Eur. J. Org. Chem.*, 2007, **2007**, 1001.

32 F. Bohlmann, H. Schönowsky, E. Inhoffen and G. Grau, *Chem. Ber.*, 1964, **97**, 794; A. Lei, M. Srivastava and X. Zhang, *J. Org. Chem.*, 2002, **67**, 1969.

33 W. A. Chalifoux, R. McDonald, M. J. Ferguson and R. R. Tykwinski, *Angew. Chem. Int. Ed.*, 2009, **48**, 7915.

34 For a detailed development of the synthesis procedure, see Supporting Information.

35 D. Heymann, *Carbon*, 2005, **43**, 2235.

36 R. H. Baughman, *Science*, 2006, **312**, 1009.

37 There is an alternative situation to also consider here: $H–[C≡C]_x–H + H–[C≡C]_y–H \rightarrow H–[C≡C]_x–[C≡C]_y–H$ Because acidity/reactivity of polyynes increases as a function of length (see ref 32), the rate of this process could be even faster than that of eqs 1–3, but would usually lead to decomposition of the products **H[*n*]** with CA. *n* > ca. 6 (see ref 9).

38 In experiments where this step was skipped, significant amounts of an insoluble, black precipitate were formed, which hampered the following workup.

39 S. Frankenberger, Diploma thesis, Friedrich-Alexander-Universität Erlangen-Nürnberg, 2010.

40 S. Eisler, A. D. Slepkov, E. Elliott, T. Luu, R. McDonald, F. A. Hegmann and R. R. Tykwinski, *J. Am. Chem. Soc.*, 2005, **127**, 2666.

41 T. Gibtner, F. Hampel, J. P. Gisselbrecht and A. Hirsch, *Chem. Eur. J.*, 2002, **8**, 408.

42 R. R. Tykwinski, W. Chalifoux, S. Eisler, A. Lucotti, M. Tommasini, D. Fazzi, M. Del Zoppo and G. Zerbi, *Pure Appl. Chem.*, 2010, **82**, 891.

43 H. Meier, U. Stalmach and H. Kolshorn, *Acta Polym.*, 1997, **48**, 379.

44 For a detailed mass spectrometric study of pure Tr*-polyynes, see: R. W. Kirschbaum, D. Prenzel, S. Frankenberger, R. R. Tykwinski and T. Drewello, *J. Phys. Chem. C*, 2015, **119**, 2861.

45 R. I. Gray, K. M. Luckett and J. Tellinghuisen, *J. Phys. Chem. A*, 2001, **105**, 11183.

46 As is observed for the formation of $[Cs(CsI)_n]^+$ and $[I(CsI)_n]^-$ cluster ions during laser desorption of CsI_3, which is commonly used for mass calibration of MALDI techniques, see: X. Lou, J. L. J. van Dongen, E. W. Meijer, *J. Am. Soc. Mass. Spectrom.*, 2010, **21**, 1223.

47 S. Bashir, W. I. Burkitt, P. J. Derrick and A. E. Giannakopulos, *Int. J. Mass Spectrom.*, 2002, **219**, 697.

48 Y. V. Vasil’ev, O. G. Khvostenko, A. V. Streletskii, O. V. Boltalina, S. G. Kotsiris and T. Drewello, *J. Phys. Chem. A*, 2006, **110**, 5967.

49 The change from apolar to polar solvent results in a slight red-shift of the absorbances, and peaks in the UV-vis spectra become broader with increasing polarity of the solvent. For a discussion of solvatochromism in polyynes, see: W. A. Chalifoux, M. J. Ferguson, R. McDonald, F. Melin, L. Echegoyen and R. R. Tykwinski, *J. Phys. Org. Chem.*, 2012, **25**, 69.